



Contents lists available at ScienceDirect

Bioorganic & Medicinal Chemistry Letters

journal homepage: www.elsevier.com/locate/bmcl

Tetra-substituted imidazoles as a new class of inhibitors of the p53–MDM2 interaction



Andrea Vaupel*, Guido Bold, Alain De Pover, Thérèse Stachyra-Valat, Joanna Hergovich-Lisztwan, Joerg Kallen, Keiichi Masuya, Pascal Furet*

Novartis Institutes for BioMedical Research, CH-4002 Basel, Switzerland

ARTICLE INFO

Article history:

Received 4 February 2014

Revised 13 March 2014

Accepted 15 March 2014

Available online 22 March 2014

Keywords:

Protein–protein interaction inhibitors

Structure-based design

p53

MDM2

ABSTRACT

Capitalizing on crystal structure information obtained from a previous effort in the search for non peptide inhibitors of the p53–MDM2 interaction, we have discovered another new class of compounds able to disrupt this protein–protein interaction, an important target in oncology drug research. The new inhibitors, based on a tetra-substituted imidazole scaffold, have been optimized to low nanomolar potency in a biochemical assay following a structure-guided approach. An appropriate strategy has allowed us to translate the high biochemical potency in significant anti-proliferative activity on a p53-dependent MDM2 amplified cell line.

© 2014 Elsevier Ltd. All rights reserved.

The p53 tumor suppressor protein plays a key role in the control of cellular integrity. Loss of function of the p53 gene by mutations or deletions is observed in almost 50% of all human cancer tissues. In other cancer tissues, still expressing the wild-type form, the normal function of p53 is altered by overexpression or amplification of MDM2 (or HDM2), the main negative regulator of the tumor suppressor. In this situation, MDM2 mainly functions as a p53 specific ubiquitin ligase which by binding to the N-terminal transactivation domain of p53 triggers its proteasomal degradation. Cancerous cells having elevated MDM2 levels are thus protected against p53 dependent apoptosis and cell cycle arrest mechanisms.

To restore normal p53 function in such tumor cells, one can envisage disrupting the p53–MDM2 interaction by small molecules having high affinity for the p53 binding pocket of MDM2. This attractive therapeutic concept has raised a lot of interest in anticancer drug research and some molecules exerting an anti-proliferative activity by this mechanism have entered clinical evaluation.^{1,2}

Several years ago, we initiated an effort in this direction that led to the identification of a very potent octapeptide inhibitor of the p53–MDM2 interaction incorporating non-natural amino-acids.³

* Corresponding authors. Address: Novartis, WKL-136.3.94, CH-4002 Basel, Switzerland. Tel.: +41 61 696 78 67; fax: +41 61 696 62 46 (A.V.). Address: Novartis, WKL-136.P.12, CH-4002 Basel, Switzerland. Tel.: +41 61 696 79 90; fax: +41 61 696 48 70 (P.F.).

E-mail addresses: andrea.vaupel@novartis.com (A. Vaupel), pascal.furet@novartis.com (P. Furet).

This octapeptide was designed on the basis of the available crystal structure of MDM2 in complex with a 15-mer peptide derived from the natural sequence of p53.⁴

We have pursued this effort by the search for non-peptide inhibitors of this critical protein–protein interaction. Along this line, we recently reported a structure-based design concept that led to the identification of a promising new class of small molecule inhibitors of the p53–MDM2 interaction.⁵ Key to the success of this concept was the observation that residue Val 93 occupies a central position in the p53 binding pocket of MDM2, a peculiar topological feature of this protein cavity. We realized that placement of a planar aromatic or hetero-aromatic core moiety within van der Waals distance of Val 93 afforded appropriate exit vectors to attach substituents that efficiently occupy the three essential sub-pockets of the MDM2 cleft involved in the recognition of residues Phe 19, Trp 23 and Leu 26 of the transactivation domain of p53.

Following the same concept, we have discovered a second class of p53–MDM2 interaction inhibitors that use a tetra-substituted imidazole ring as core structure. We report here the design of these compounds and the optimization of their biochemical and cellular potency.

In our previous work on the identification of 3-imidazolyl indole p53–MDM2 inhibitors based on the central valine concept, a crystal structure of MDM2 in complex with compound **1** (Fig. 1) was obtained.⁶ In this structure (Fig. 2) one observes an aromatic π – π stacking interaction between MDM2 residue His 96 and the benzylic chlorophenyl ring of the compound. We noticed that besides this stacking interaction the side chain of His 96 offered

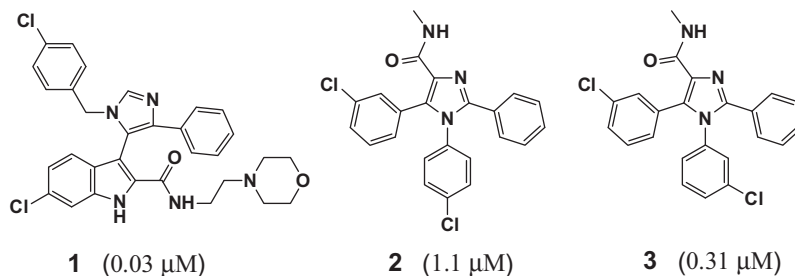


Figure 1. Chemical structures of compounds 1–3. Inhibitory activity in the TR-FRET biochemical assay is indicated in parentheses.

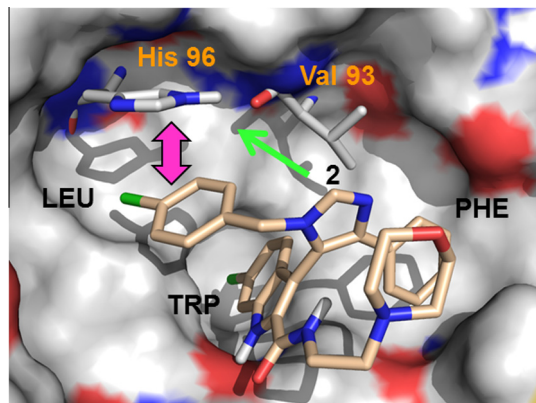


Figure 2. Crystal structure of MDM2 in complex with compound 1 (PDB code: 4DJJ). The π – π stacking interaction with His 96 and the proximity of the 2-position of the compound imidazole ring with the hydrogen bond donor nitrogen of the side chain of this residue are highlighted. The three MDM2 sub-pockets are labeled PHE (Phe 19), TRP (Trp 23) and LEU (Leu 26).

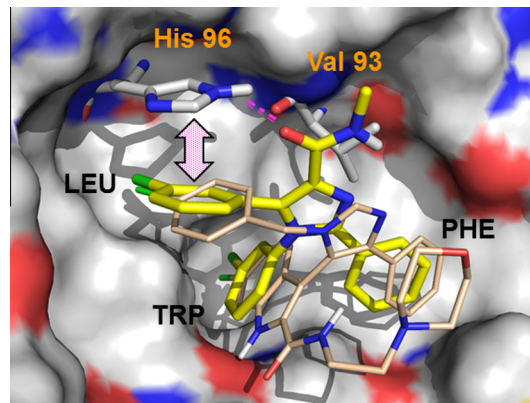


Figure 3. The design of the prototype compounds is illustrated here by a model of compound 3 (yellow) binding in the MDM2 pocket. The model is based on the crystal structure of MDM2 in complex with compound 1 (PDB code: 4DJJ). Compound 1 (beige) is also represented as reference. For compound 3, the putative hydrogen bond formed with His 96 appears as a dashed pink line while the putative π – π stacking interaction is represented by the dashed pink arrow.

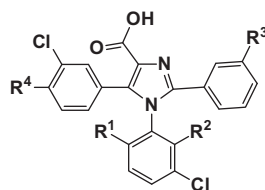
the possibility to form a hydrogen bond with the inhibitor. Closer examination of the crystal structure suggested creating this new interaction by placing a hydrogen bond accepting group in position 2 of the imidazole ring of **1**.⁷ In particular, in one molecular modeling experiment, we probed an amide group directly attached at this position of the imidazole ring to interact with His 96. However, in the resulting model the amide oxygen atom was too far from the side chain imidazole ring of His 96 to actually form a hydrogen bond. Further modeling experiments indicated that this hydrogen bond could be created if two other modifications of the 3-imidazolyl indole inhibitor were made: firstly replace the indole moiety by a *para*- or *meta*-chlorophenyl ring to fill the Trp 23 sub-pocket and secondly replace the benzylic group by a *meta*-chlorophenyl ring directly attached to the imidazole core for stacking with His 96. These modifications allowed the formation of the targeted hydrogen bond by a slight motion of the molecule towards His 96 upon energy minimization (Fig. 3).⁸ After consideration of synthetic access, we settled on prototype molecules **2** and **3** (Fig. 1) to probe the idea of engaging His 96 for both a π – π stacking and hydrogen bond interaction while conforming to our central valine ligand design concept.

Compounds **2** and **3** were synthesized and tested in our biochemical TR-FRET assay measuring the ability of a compound to inhibit the binding of a p53-derived peptide to MDM2.⁹ Gratifyingly, with IC_{50} values of 1.1 and 0.31 μM respectively, **2** and **3** showed significant activity in this assay. The encouraging sub-micromolar activity of **3** incited us to also test its carboxylic acid synthetic intermediate **4** (Table 1). The latter compound turned out to be 3-fold more potent than **3**. The observed improvement was consistent with our hypothesis that the prototype compounds establish a hydrogen bond with the side chain imidazole ring of His 96, a

strengthening of this interaction being expected as the consequence of replacing a neutral hydrogen bond acceptor group by an ionized negatively charged one. These promising results prompted us to initiate a chemistry program aimed at optimizing the potency of the new chemotype with compound **4** as the starting point.

Guided by our model of the compound docked in the MDM2 cavity (Fig. 4), we designed several modifications of **4** with the objective of either enhancing its conformational preorganization for MDM2 binding or improving its interactions with the protein. This effort resulted in the synthesis of compounds **5**–**8** (Table 1). Concerning the former aspect, we noticed that in the binding model (Fig. 4) the *meta*-chlorophenyl ring of **4** occupying the Trp 23 sub-pocket had a nearly perfect perpendicular orientation with respect to the plane of the core imidazole ring. However, when the compound was energy minimized outside the cavity, the angle between the two ring planes was smaller assuming a value of 50°. ¹⁰ To stabilize the higher energy perpendicular conformation induced by the cavity, we envisaged the introduction of substituents at the positions of the chlorophenyl ring *ortho* to its attachment point. Modeling suggested that either a methyl group at the 6-position or a fluorine atom at the 2-position of the ring would facilitate, by intramolecular steric hindrance, the full deconjugation of the chlorophenyl and imidazole rings without creating adverse interactions with the binding site. It was expected that the 6-methyl substituent would face solvent while the 2-fluorine atom would increase the favorable contact surface area with MDM2 through additional hydrophobic interactions with residues Val 93, Phe 91 and Ile 99. Remarkably, with compounds **5** and **6**, designed on the basis of this concept, the biochemical potency of **4** could be improved 11- and 17-fold, respectively. We sought to further increase

Table 1
Biochemical and cellular activity of compounds 4–8



Compound	R ¹	R ²	R ³	R ⁴	TR-FRET IC ₅₀ (μM)	SJSA-1 IC ₅₀ (μM)	SAOS-2 IC ₅₀ (μM)
4	H	H	H	H	0.12	n.d.	n.d.
5	Methyl	H	H	H	0.011	16.1	>30
6	H	F	H	H	0.007	12.2	>30
7	Methyl	H	Methyl	H	0.008	10.2	>30
8	H	F	H	F	0.003	14.0	>30

The IC₅₀ values are averages of at least 2 separate determinations.

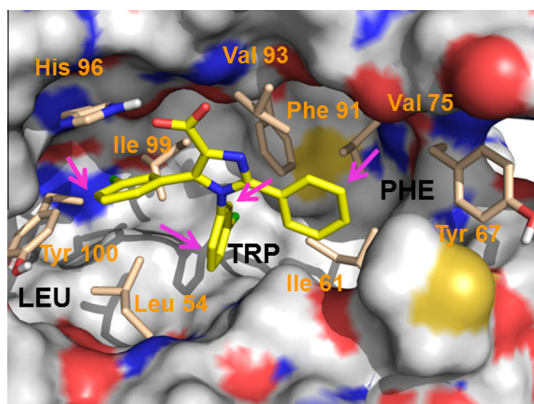


Figure 4. Binding model of compound 4 (yellow) in the MDM2 pocket. The positions of the compound where substituents were introduced to enhance its potency are indicated by pink arrows.

the inhibitory activity of these first nanomolar compounds of the series by optimizing interactions in the Phe 19 and Leu 26 sub-pockets of MDM2. Two modifications were designed to this end based on the docking model. On the one hand, we introduced a methyl group in *meta* position of the phenyl ring interacting with the Phe 19 sub-pocket. This substituent was meant to fill a small empty hydrophobic space left in this part of the cavity between the side chains of residues Ile 61, Tyr 67 and Val 75. On the other hand, a fluorine atom was added at the 4-position of the chlorophenyl ring occupying the Leu 26 sub-pocket to make favorable van der Waals contacts with the side chains of residues Leu 54 and Tyr 100. Compounds 7 and 8 are representative of these designs. Comparing the biochemical IC₅₀ values of the pairs 5, 7 and 6, 8 indicates that, as expected, some gain in binding affinity, although modest, was achieved by seeking additional interactions in the Phe 19 and Leu 26 sub-pockets. With compound 8, low single digit nanomolar potency was thus reached. In addition, compound 7 provided the first success in our attempts to obtain an X-ray crystal structure of MDM2 in complex with a member of the new chemotype series.¹¹ As shown in Figure 5, this structure fully validated the design principles used for the identification of the new class of p53–MDM2 inhibitors. The π – π stacking interaction between the *meta*-chlorophenyl ring and His 96 is indeed observed in the Leu 26 sub-pocket. So is the hydrogen bond between this residue and the carboxylic acid group in position 4 of the compound imidazole ring.¹² Moreover, the binding mode of 7 overall

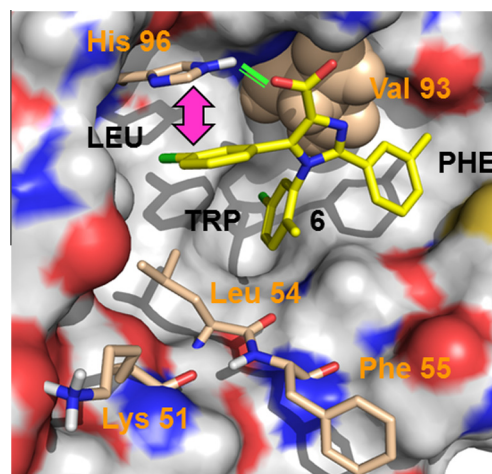


Figure 5. Crystal structure of MDM2 in complex with compound 7 (PDB code: 4OQ3). The side chain of the central valine 93 is shown in CPK representation. The hydrogen bond and π – π stacking interactions with His 96 are indicated in green and pink colors, respectively. As expected from the docking models, the plane of the inhibitor core imidazole ring and that of its chlorophenyl ring occupying the Trp 23 sub-pocket are nearly perpendicular, an angle of 80° being observed. MDM2 residues Lys 51, Leu 54 and Phe 55 facing position 6 of the latter chlorophenyl ring appear in stick representation.

conforms to our central valine concept with the imidazole ring of the compound in van der Waals interaction with residue Val 93 and the three attached phenyl groups projecting in the three crucial p53 binding sub-pockets of MDM2.

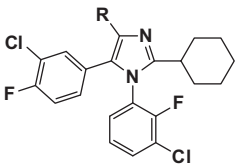
Having obtained very potent inhibitors of the p53–MDM2 interaction at the biochemical level, we next turned our attention to the optimization of cellular activity. We assessed it by measuring the ability of compounds to inhibit the proliferation of SJSA-1 cells. These are p53 positive cancer cells in which the MDM2 gene is amplified. For control, inhibition of the proliferation of the p53-null SAOS-2 cells was also measured.¹³

We were pleased to note that compounds 5–8 (Table 1) showed inhibition of the proliferation of the p53-dependent SJSA-1 cells while having no effect on the p53-null SAOS-2 cells in the same range of concentrations. However, limited to the double digit micromolar level, this inhibition was weak in sharp contrast with the high biochemical potency achieved. Although p53–MDM2 inhibitors are expected to lose potency going from a biochemical to a cellular setting because of the existence of the p53–MDM2

auto-regulatory feedback loop in cells,¹⁴ we believed that the presence of a carboxylic acid group in the compounds, by hampering their cell permeability, could be an important contributor to the observed discrepancy. To explore this possibility, we envisaged bioisosteric replacements of the carboxylic acid group. Since, in the perspective of ADME properties optimization, we also wanted to reduce aromaticity in our lead series, replacement of the carboxylic group was carried out on **9** (Table 2), the analogue of **8** in which the phenyl group fitting the Phe 19 sub-pocket was replaced by a cyclohexyl ring. A docking experiment suggested that such a modification would be tolerated and indeed **9** turned out to be as potent as **8**, both in the biochemical and cellular assay.

The carboxylic acid in **9** was first converted to a primary amide to give compound **10** (Table 2). As expected, this alteration caused a drop in biochemical potency because of the weakening of the hydrogen bond formed with the side chain of His 96. Nevertheless, the desired improvement in cellular activity was obtained, compound **10** having an IC₅₀ value of 4.1 μM in the SJS-A1 proliferation assay compared to a value of 13.2 μM for **9**. We next tried the classical tetrazole carboxylic acid isostere. The resulting compound **11**, being able to interact with His 96 in an ionized form, regained potency in the TR-FRET assay compared to **10** but was not more active at the cellular level. Going back to a neutral group as carboxylic acid substitute, a 2-methyl-1,3,4-oxadiazole ring was designed (compound **12**).¹⁵ In the binding model, one of the ring nitrogen atoms could establish the hydrogen bond with His 96. Again, replacement of the carboxylic acid by a neutral isostere led to a reduction of biochemical potency while improving activity in the cellular assay. Reasoning that a strong electron donating substituent on the oxadiazole ring would make the nitrogen atom interacting with His 96 a better hydrogen bond acceptor, we synthesized compound **13**. Consistent with this notion, **13** showed enhanced biochemical activity compared to **12**, reaching the low nanomolar levels of **9** or **11**. In addition, with an IC₅₀ value of 3.5 μM, **13** represented the most potent compound of the series in the SJS-A1 proliferation assay.

Table 2
Biochemical and cellular activity of compounds **9–13**



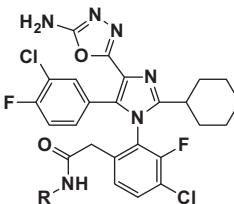
Compound	R	TR-FRET IC ₅₀ (μM)	SJS-A1 IC ₅₀ (μM)	SAOS-2 IC ₅₀ (μM)
9		0.004	13.2	>30
10		0.018	4.1	29
11		0.003	4.4	>30
12		0.025	5.9	>30
13		0.006	3.5	>30

The IC₅₀ values are averages of at least 2 separate determinations.

Consequently, compound **13** was selected as the starting point for a new round of cellular potency optimization. Looking for ways to further improve the intrinsic binding affinity of the compound for MDM2 that might translate in better cellular activity, we noticed that extending a side chain from position 6 of the phenyl moiety occupying the Trp 23 sub-pocket allowed the creation of interactions with residues Leu 54, Lys 51 and Phe 55 (see Fig. 5). In particular, with an acetamide group attached to this position, it was possible to form a hydrogen bond with the backbone carbonyl group of Leu 54, recapitulating an interaction made by the side chain of the p53 residue Trp 23. **14** was the first compound synthesized following this concept. Besides this methyl derivative, analogues bearing a larger substituent on the amide group (compounds **15–17**) were also prepared to target the side chains of the three aforementioned residues for hydrophobic interactions. From the data in Table 3 it can be seen that this strategy met with some success, three compounds of the series, those having an aliphatic substituent (**14**, **16** and **17**), being more active both biochemically and cellularly than the parent compound **13**. Importantly, the *tert*-butyl derivative **17** reached sub-micromolar potency (IC₅₀ = 0.5 μM) in the SJS-A1 proliferation assay, comparing favorably with the micromolar activity (IC₅₀ = 1.9 μM) of the well established p53–MDM2 inhibitor Nutlin-3a in this assay.

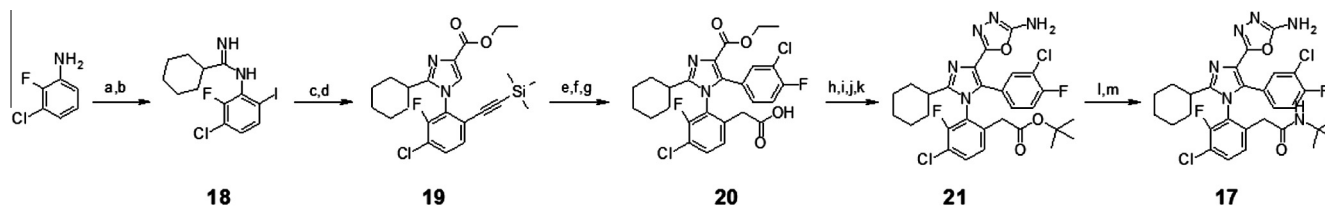
A representative synthesis for compound **17** is shown in Scheme 1.¹⁶ Commercially available 2-fluoro-3-chloro aniline was subjected to iodination with NIS, providing a regioisomeric mixture of 4- and 6-iodo products which were separable by flash chromatography. The desired 6-iodo regioisomer was reacted with cyclohexane carbonitrile in the presence of trimethyl aluminum to form the corresponding benzimidazole **18** which underwent a smooth cyclization with ethylbromo pyruvate under mild basic conditions (NaHCO₃; rt). Water elimination was effected by addition of *p*-toluene sulfonic acid and heating to 120 °C to furnish the imidazole core. Selective Sonogashira coupling of the iodine with trimethyl silyl acetylene provided intermediate **19**. Conversion of the acetylene side chain to the desired acid was achieved by hydroboration (cyclohexene/borane-dimethylsulfide complex) and oxidative workup. Efficient and selective bromination of the imidazole core was effected by treatment with NBS in acetonitrile at room temperature, providing the suitable substrate for a Suzuki coupling with commercially available 3-chloro-4-fluoro boronic acid. Orthogonal ester protection/deprotection steps provided acid **20** which was converted to the 2-amino-oxadiazole in a two steps sequence (HATU promoted hydrazone formation and ring closure with BrCN). Finally deprotection of the *tert*-butyl ester **21** liberates carboxylic acid which was converted to the corresponding carboxamide **17** using Propasal™ as a coupling reagent.

Table 3
Biochemical and cellular activity of compounds **14–17**



Compound	R	TR-FRET IC ₅₀ (μM)	SJS-A1 IC ₅₀ (μM)	SAOS-2 IC ₅₀ (μM)
14	Methyl	0.004	1.4	24
15	Phenyl	0.006	2.5	30
16	Cyclohexyl	0.002	1.4	28
17	<i>tert</i> -Butyl	0.002	0.5	23

The IC₅₀ values are averages of at least 2 separate determinations.



Scheme 1. Reactions and conditions: (a) NIS, CH_2Cl_2 , rt, **5d**; (b) cyclohexane carbonitrile, Me_3Al , toluene, 110 °C; (c) (1) ethyl bromopyruvate, NaHCO_3 , rt, 2 h, (2) p-TSA, toluene, 120 °C, 1 h; (d) trimethylsilylacetylene, $\text{Pd}(\text{OAc})_2$, PPh_3 , NEt_3 , rt, 20 h; (e) (1) cyclohexene, $\text{Me}_2\text{S}\cdot\text{BH}_3$, THF, rt, 3 h, (2) NaHCO_3 , H_2O_2 , THF, rt; (f) NBS, CH_3CN , rt, 8 h; (g) 3-chloro,4-fluoro phenylboronic acid, $\text{Pd}(\text{PPh}_3)_4$, K_3PO_4 , dioxane/ H_2O , 100 °C, 18 h; (h) *tert*-butyl 2,2,2-trichloroacetimidate, $\text{BF}_3\cdot\text{Et}_2\text{O}$, CH_2Cl_2 /cyclohexene, rt, 3 h; (i) LiOH, H_2O /dioxane, 70 °C, 3 h; (j) hydrazine, HATU, *N*-methylmorpholine, DMF, rt, 2 h; (k) BrCN, NaHCO_3 , H_2O /dioxane, rt, 6 h; (l) HCl/dioxane, rt, 3 days; (m) *tert*-butyl amine, Propal™, NEt_3 , DMAP, DMF, rt, 2 h.

In conclusion, building on our previous work on the discovery of 3-imidazolyl indole inhibitors of the p53–MDM2 interaction, we have identified by structure-based design another new class of inhibitors of this interaction. By appropriate derivatization strategies guided by structural information, we were able to optimize the MDM2 affinity of these tetra-substituted imidazole inhibitors to the low nanomolar range. The most potent compounds of the series show significant and specific anti-proliferative activity in cultures of p53-dependent cancer cells. These results warrant further evaluation of the new inhibitors towards the goal of developing anti-cancer agents to fight tumors harboring an overexpressed or amplified MDM2 gene.

References and notes

- For recent reviews on the topic see: (a) Wade, M.; Li, Y. C.; Wahl, G. M. *Nat. Rev. Cancer* **2013**, *13*, 83; (b) Li, Q.; Lozano, G. *Clin. Cancer Res.* **2013**, *19*, 34; (c) Carry, J. C.; García-Echeverría, C. *Bioorg. Med. Chem. Lett.* **2013**, *23*, 2480; (d) Wang, S.; Zhao, Y.; Bernard, D.; Aguilar, A.; Kumar, S. *Top. Med. Chem.* **2012**, *8*, 57; (e) Capdevila, J.; Cervantes, A.; Tabernero, J. *Drugs Future* **2012**, *37*, 273; (f) Ray-Coquard, L.; Blay, J. Y.; Italiano, A.; LeCesne, A.; Penel, N.; Zhi, J.; Heil, F.; Rueger, R.; Graves, B.; Ding, M.; Geho, D.; Middleton, S. A.; Vassilev, L. T.; Nichols, G. L.; Bui, B. N. *Lancet Oncol.* **2012**, *13*, 1133; (g) Macchiarulo, A.; Giacchè, N.; Carotti, A.; Moretti, F.; Pellicciari, R. *Med. Chem. Commun.* **2011**, *2*, 455; (h) Cheok, C. F.; Verma, C. S.; Baselga, J.; Lane, D. P. *Nat. Rev. Clin. Oncol.* **2011**, *8*, 25; (i) Millard, M.; Pathania, D.; Grande, F.; Xu, S.; Neamati, N. *Curr. Pharm. Des.* **2011**, *17*, 536; (j) Brown, C. J.; Cheok, C. F.; Verma, C. S.; Lane, D. P. *Trends Pharmacol. Sci.* **2011**, *32*, 53; (k) Vu, B. T.; Vassilev, L. In *Current Topics in Microbiology and Immunology (Small Molecules Inhibitors of Protein-Protein Interactions)*; Vassilev, L., Fry, D., Eds.; Springer-Verlag: Berlin Heidelberg, 2011; Vol. 348, pp 151–172; (l) Weber, L. *Expert Opin. Ther. Patents* **2010**, *20*, 179; (m) Zak, K.; Pecak, A.; Rys, B.; Wladyka, B.; Doemling, A.; Weber, L.; Holak, T. A.; Dubin, G. *Expert Opin. Ther. Patents* **2013**, *23*, 425.
- For recent papers see: (a) Ding, Q.; Zhang, Z.; Liu, J.; Jiang, N.; Zhang, J.; Ross, T. M.; Chu, X. J.; Bartkowitz, D.; Podlaski, F.; Janson, C.; Tovar, C.; Filipovic, Z.; Higgins, B.; Glenn, K.; Packman, K.; Vassilev, L.; Graves, B. *J. Med. Chem.* **2013**, *56*, 5979; (b) Miyazaki, M.; Naito, H.; Sugimoto, Y.; Yoshida, K.; Kawato, H.; Okayama, T.; Shimizu, H.; Miyazaki, M.; Kitagawa, M.; Seki, T.; Fukutake, S.; Shiose, Y.; Aonuma, M.; Soga, T. *Bioorg. Med. Chem.* **2013**, *21*, 4319; (c) Gonzalez-Lopez de Turiso, F.; Sun, D.; Rew, Y.; Bartberger, M. D.; Beck, H. P.; Canon, J.; Chen, A.; Chow, D.; Correll, T. L.; Huang, X.; Julian, L. D.; Kayser, F.; Lo, M. C.; Long, A. M.; McMinn, D.; Oliner, J. D.; Osgood, T.; Powers, J. P.; Saiki, A. Y.; Schneider, S.; Shaffer, P.; Xiao, S. H.; Yakowec, P.; Yan, X.; Ye, Q.; Yu, D.; Zhao, X.; Zhou, J.; Medina, J. C.; Olson, S. H. *J. Med. Chem.* **2013**, *56*, 4053; (d) Tovar, C.; Graves, B.; Packman, K.; Filipovic, Z.; Higgins, B.; Xia, M.; Tardell, C.; Garrido, R.; Lee, E.; Kolinsky, K.; To, K.-H.; Linn, M.; Podlaski, F.; Wovkulich, P.; Vu, B.; Vassilev, L. T. *Cancer Res.* **2013**, *73*, 2587; (e) Vu, B.; Wovkulich, P.; Pizzaloloto, G.; Loveley, A.; Ding, Q.; Jiang, N.; Liu, J.-J.; Zao, C.; Glenn, K.; Wen, Y.; Tovar, C.; Packman, C.; Vassilev, L.; Graves, B. *ACS Med. Chem. Lett.* **2013**, *4*, 466; (f) Zhao, Y.; Yu, S.; Sun, W.; Liu, L.; Lu, J.; McEachern, D.; Shargary, S.; Denzil, B.; Li, X.; Zhao, T.; Zou, P.; Sun, D.; Wang, S. *J. Med. Chem.* **2013**, *56*, 5533.
- García-Echeverría, C.; Chêne, P.; Blommers, M. J. J.; Furet, P. *J. Med. Chem.* **2000**, *43*, 3205.
- Kussie, P. H.; Gorina, S.; Marechal, V.; Elenbaas, B.; Moreau, J.; Levine, A. J.; Pavletich, N. P. *Science* **1996**, *274*, 948 (PDB code: 1YCR).
- Furet, P.; Chêne, P.; De Pover, A.; Stachyra-Valat, T.; Hergovich-Lisztwan, J.; Kallen, J.; Masuya, K. *Bioorg. Med. Chem. Lett.* **2012**, *22*, 3498.
- The PDB code of this crystal structure is 4DIJ.
- We assumed that in the crystal structure the Nε2 nitrogen atom of the side chain of His 96 is protonated because it is within hydrogen bond distance of the backbone carbonyl oxygen atom of Val 93.
- Modeling and docking were performed with a version of MacroModel enhanced for graphics by A. Dietrich. MacroModel: Mohamadi, F.; Richards, N. G. J.; Guida, W. C.; Liskamp, R.; Lipton, M.; Caufield, C.; Chang, G.; Hendrickson, T.; Still, W. C. *J. Comput. Chem.* **1990**, *11*, 440. The compounds were manually constructed and docked in the MDM2 pocket (PDB structure 4DIJ) and the resulting ligand-protein complexes energy-minimized using the AMBER⁷/H₂O/GBSA force field.
- For a detailed description of the TR-FRET (Time Resolved Fluorescence Resonance Energy Transfer) biochemical assay used see: Berghausen, J.; Buschmann, N.; Furet, P.; Gessier, F.; Hergovich Lisztwan, J.; Holzer, P.; Jacoby, E.; Kallen, J.; Masuya, K.; Pissot Soldermann, C.; Ren, H.; Stutz, S. PCT Int. Appl. WO 2011076786, 2011; *Chem. Abstr.* **2011**, *155*, 152537. In this assay the donor fluorophore is MDM2 (amino acid residues 2–188) tagged with a C-terminal biotin moiety in combination with a Europium labeled streptavidin. The acceptor fluorophore is a p53 derived peptide (amino acid sequence 18–26 of p53: TFSDLWKLK) labeled with the fluorescent dye Cy5. The IC₅₀ values given are means of at least two measurements. For reference, the p53–MDM2 inhibitor Nutlin-3A has an IC₅₀ of 0.01 μM in this assay.
- The minimization of the isolated molecule was performed in MacroModel using the AMBER⁷/H₂O/GBSA force field.
- Kallen, J. Crystallographic coordinates and structural factors of compound **7** in complex with the N-terminal domain of MDM2 have been deposited with the Protein Data Bank (entry code 4OQ3). The structure was solved at 2.3 Å resolution.
- A search in the Protein Data Bank indicates that other classes of p53–MDM2 inhibitors originating from independent efforts are able to form these beneficial interactions with His 96. Both the stacking interaction and the hydrogen bond are observed in PDB structures 4HBM, 4ERE, 4ERF, 4OAS (Amgen piperidinone inhibitors) and 4JVR, 4JSC (Roche spiroindoline inhibitors) while the stacking interaction only is observed in structures 3JZK (Amgen chromenotriazolopyrimidine inhibitors) and 1T4E (Johnson & Johnson benzodiazepinedione inhibitors).
- The cellular SJS-1 and SAOS-2 proliferation assays are based on YO-PRO[®]-1 iodide staining (*J. Immunol. Methods* **1995**, *185*, 249). To test the effect of compounds on cell growth, SJS-1 cells (p53 wild-type cells) and SAOS-2 cells (p53 null cells) are plated out into 96-well micro-titer plates and treated with decreasing concentrations of the compounds. After a 72 h incubation period, 2.5 μM YO-PRO[®]-1 iodide is directly added to the cells and a first read-out is performed using a standard fluorescence plate reader (filter setting 485/530 nm) revealing the relative number of apoptotic cells. Subsequently, cells are permeabilized by directly adding lysis buffer containing the detergent NP40, EDTA and EGTA to obtain final concentrations of 0.01% and 5 mM, respectively. After complete permeabilization, the total cell number is quantified during a second read using the fluorescence plate reader with the same settings.
- Lahav, G. In *Cellular Oscillatory Mechanisms*; Maroto, M., Monk, N. A. M., Eds.; Landes Bioscience and Springer Science, 2008; pp 28–38.
- Bergström, J.; Hogner, A.; Llinàs, A.; Wellner, E.; Plowright, A. T. *J. Med. Chem.* **2012**, *55*.
- The preparation of the compounds presented in this work is detailed. In: Bold, G.; Furet, P.; Kallen, J.; Hergovich Listwan, J.; Masuya, K.; Vaupel, A. PCT Int. Appl. WO 2011023677.